Article

Adjustable Overtopping Wave Energy Converter by Using Smart Material

Sina Baghbani Kordmahale[1], Chia-Hung Chien[2], Jun Kameoka[1] and Kuang-An Chang[2, 3, *]

[1] Department of Electrical and Computer Engineering, Texas A&M University, College Station, Texas, USA
[2] Department of Ocean Engineering, Texas A&M University, College Station, Texas, USA
[3] Zachry Department of Civil Engineering, Texas A&M University, College Station, Texas, USA
* Correspondence: kchang@tamu.edu

Abstract

A Shape Memory Alloy (SMA) enabled Overtopping Wave Energy Converter (OWEC) that maximizes its overtopping discharge, and thus energy output under different wave conditions is presented. Among all the parameters affecting the overtopping discharge rate, the crest freeboard height is the most influential one to control the overtopping discharge rate and the stored overtopping volume behind it. Currently, all the OWEC crest freeboard heights are fixed by design to maximize the discharge rate on one particular sea state. In the present study, we show that the SMA can adjust the crest freeboard height through a control system based on the sea state and achieve an optimal overtopping discharge rate. A scaled OWEC model is built in the lab with its crest freeboard height controlled by springs made of SMA. The length (and thus tension) of the springs is controlled by temperature changes by changing the passing current through the springs. By adjusting the length of the springs based on the incoming wave condition, we adjust the freeboard to an optimal height known to generate a maximum overtopping discharge rate for energy conversion. This smart material-enabled design can maximize the overtopping discharge and thus the output power of the OWEC under various wave conditions. Furthermore, the simplicity of using SMA springs as the actuator leads to the minimum number of moving mechanical parts, which can remarkably decrease maintenance costs. As the proof of concept, two types of tests are conducted in the laboratory using the same OWEC model under several random wave trains generated from spectra with different significant wave heights - one type with a fixed crest freeboard height and the other type featuring the adjustable crest freeboard height controlled by the springs. The substantial increase of harvested output power in the OWEC with the adjustable crest freeboard height may pave the way for more efficient wave energy conversion systems.

Keywords: Wave energy converter; Wave overtopping; Shape memory alloy; Random waves

1. Introduction

Renewable clean energies have received massive attention as a substitute for fossil fuels because of both environmental and economic considerations. The abundance of ocean waves makes wave energy a candidate for sustainable green energy. There are many types of Wave Energy Converter (WEC) that can convert the mechanical motion of waves to electrical power [1,2]. However, the conversion efficiencies are mostly low while the costs are high when compared to the traditional fossil fuel-based power sources. As a result, tremendous efforts have been devoted to improving the efficiency of wave power harnesses.

Preprints (www.preprints.org) | NOT PEER-REVIEWED | Posted: 8 November 2022 doi:10.20944/preprints202211.0143.v1

The Overtopping Wave Energy Converter (OWEC) is one type of existing wave energy converter that converts potential energy that is stored in a reservoir behind the freeboard of the converter. The stored water in the reservoir is from the generated discharge produced by wave overtopping the converter. Since the water level in the reservoir is higher than the sea water level (SWL), turbines inside the converter begin to rotate due to the outflow and generate electricity. The most classical floating device of this type is perhaps the Wave Dragon which has been prototyped and is in operation. While researchers have been investigating and improving its conversion efficiency, the ratio of energy conversion, defined as the average electric power generated by the operating turbines to the theoretical incoming wave power, is only around 10% [3]. Improving the conversion efficiency is thus crucial if this type of converter is to become feasible and practical. There are two ways to increase the efficiency of OWECs in the production of electricity. The first approach is to use a more efficient power converter to convert the saved potential energy in an OWEC into electricity, while the second approach is to improve the overtopping discharge rate of the harvesters in the way of maximizing the stored overtopping volume. The present study mainly focuses on the later. To examine the overtopping discharge rate and efficiency of an OWEC device, scaled experimental tests are typically performed because of the complexity and the non-linear nature of the wave overtopping phenomenon.

Originally, overtopping structures, such as dikes, were built for coastal defense so that the goal is to minimize the overtopping discharge by preventing the sea water from reaching and flowing through the top of the structures. However, the goal of OWECs is exactly opposite - their goal is to collect more sea water from overtopping and store the water in the reservoir behind the dike. That means the height of the dikes equivalent of OWECs is as low as possible to be able to generate more overtopping discharge but as high as possible to be able to store more water behind them. An optimization process to determine the height of the dikes has thus been studied to maximize the volume flowrate stored for subsequent energy conversion based on the site-specific wave environment.

There are several factors affecting the overtopping discharge rate of OWEC. They can be divided into two categories: (i) environment factors and (ii) construction factors. For the environmental factors, the most influential one is wave climates such as the directions of waves and the shapes of the wave power spectra relevant to the conversion of mechanical motions to electrical power. The construction factors include the engineering control of the system and properties of the sloped ramp, such as the roughness, permeability, height, and angle. Naturally, an increase in roughness and permeability of the ramp slope decreases the overtopping rate. Several investigations have found that different kinds of armor units provide different roughness and porosity [4-7]. Furthermore, the slope angle also affects the overtopping rate. It has already been found that there is no significant change when the slopes vary from 35° to 50°, while if the slop is increased to 60° the overtopping would be decreased to 70% ~ 80% in comparison to a slope of 40° [8,9].

In addition to the aforementioned structural parameters, the most influential structural parameter is the freeboard crest height (R_c) which is defined as the vertical distance between the freeboard crest and the SWL. R_c affects not only the flowrate of the wave overtopping but also the volume of water stored. A larger R_c increases the capacity of the reservoir of the OWEC, while it makes waves harder to overtop. In contrast, a small R_c allows a high overtopping flowrate but decreases the reservoir capacity. Thus, research was performed to change the R_c value to adapt different wave conditions and achieve higher wave-power conversion efficiencies. Previous studies used two methods to change R_c. The first one is by changing the slope angle (α) of the ramp using a

Preprints (www.preprints.org) | NOT PEER-REVIEWED | Posted: 8 November 2022 doi:10.20944/preprints202211.0143.v1

hinge at the bottom of the slope. However, changing α may also dramatically decrease the discharge [10]. The other one is by controlling the floating height of the device using a Programmable Logic Controller (PLC). PLC controls blowers and the valves under the device to regulate the buoyancy. The regulation allows the ramp to rise in a storm so that power capture can be improved [11]. However, this method also changes the draft that adversely delimits energy takeoff from the water column. As it is discussed, these two methods are unable to adjust R_c independently without adverse effects on power conversion efficiency.

The objective of the present study is to develop a new approach to optimizing the overtopping flowrate by changing R_c without the adverse effects of changing other influential parameters, such as the ramp angle and draft. A Shape Memory Alloy-based (SMA-based) actuator is used to adjust the length of the ramp. SMA has the capability of lifting more than 100 times of its weight in a proper design [12] and has been used widely in making actuators [13]. SMA is a lower cost, smaller, and easier to use when working as small motors or solenoids, and is reliable to obtain repeatable motion for tens of millions of cycles with an appropriate design [14,15]. In this designed OWEC, 46 parallel springs made of SMA were used as the actuator with their length controlled by applying an electric current. The operating mechanism is joul heating so that the temperature of the springs is changed by turning on/off the electric current. As a result, the length of the springs became shorter or elongated to the desired length by controlling the temperature of the SMA springs; this is in turn used to control R_C. This novel idea of using SMA on an OWEC was implemented in a physically-scaled laboratory model and tested in a wave flume. Also, the results of the experiment were analyzed and compared with results of other similar tests with a fixed R_c.

2. Model Development and Experimental Setup

2.1. General overtopping flowrate

To predict and quantify the overtopping discharge rate of a coastal structure or equivalent, an exponential equation has been proposed in most cases. Equation (1) shows the most widely used form[8].

$$Q = ae^{-bR} \tag{1}$$

where $Q\,(-)$ is the dimensionless overtopping discharge, $R\,(-)$ is the dimensionless crest freeboard height, which is also called relative crest freeboard height, and a and b are coefficients, which are empirically determined from experiments. Because of the different purposes between coastal protection structures and OWECs, the later has different prediction equations. As shown in Figure 1, the most obvious difference is the draft - an OWEC in general does not extend to the seabed. That influences the energy flux captured from the water column.

The following equation has been widely used to predict the overtopping rate $Q(-)$ for OWECs. It is similar to Equation (1) but featuring several additional coefficients to account for different wave conditions and different geometries of the structures [8].

$$Q = \frac{q}{\sqrt{gH_s^3}} = \lambda_{dr}\lambda_{\alpha}\lambda_s 0.2e^{-2.60\frac{R}{\gamma}} \tag{2}$$

Preprints (www.preprints.org) | NOT PEER-REVIEWED | Posted: 8 November 2022 doi:10.20944/preprints202211.0143.v1

where q (m^2/s) is the mean overtopping discharge per unit width, H_s (m) is the significant wave height, γ (−) is the reduction coefficient which equals to unity if there are no berms, shallow foreshores, roughness, and angles of wave attack. The coefficients λ_{dr}, λ_α, and λ_s are related to drafts, slope angles, and crest freeboards, respectively, as defined in Equations (3-5) below[8].

$$\lambda_{dr} = 1 - 0.4 \frac{\sinh\left[2k_p d\left(1-\frac{d_r}{d}\right)\right] + 2k_p d\left(1-\frac{d_r}{d}\right)}{\sinh\left(2k_p d\right) + 2k_p d} \quad (3)$$

$$\lambda_\alpha = \left[\cos\left(\alpha - 30\right)\right]^3 \quad (4)$$

$$\lambda_s = \begin{cases} 0.4\sin\left(\frac{2\pi R}{3}\right) + 0.6 & \text{for } R < 0.75 \\ 1 & \text{for } R \geq 0.75 \end{cases} \quad (5)$$

where k_p is the wave number corresponding to the peak period (T_p), d_r is the draft of the structure, d is the water depth, α is the slope angle of the structure ramp, and R is the relative crest freeboard height, defined as the ratio of the crest freeboard height to the significant wave height (i.e., $R = R_c/H_s$). Hence, these three coefficients (λ_{dr}, λ_α, and λ_s) are determined based on the construction of the structure and the designed wave condition. With the determined coefficients, the prediction equation can be applied to estimate the designed overtopping discharge rate.

(a)

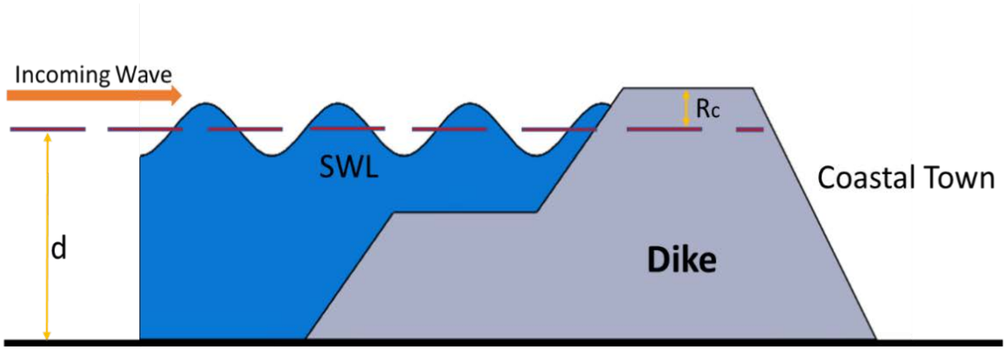

(b)

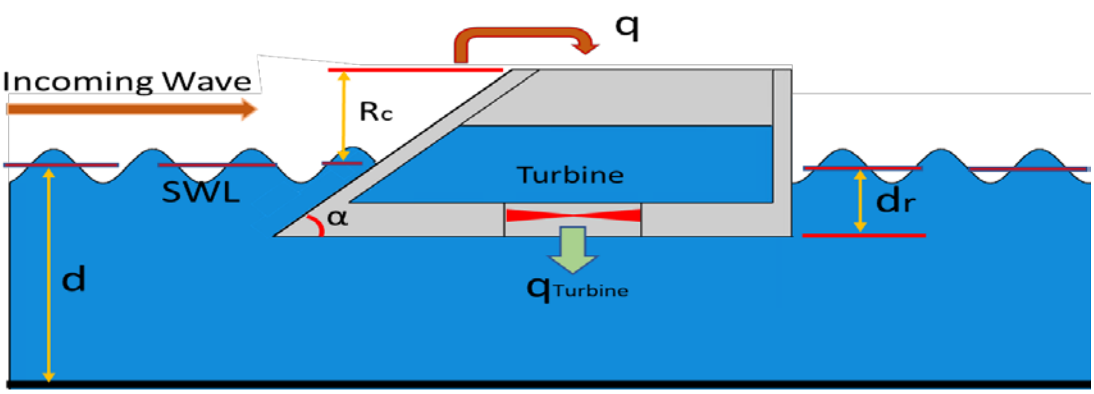

*Figure 1. **Sketches of overtopping structures** (a) Coastal dike. (b) OWEC.*

 doi:10.20944/preprints202211.0143.v1

2.2. OWEC model setup

In the present study, a scaled physical OWEC model was built and tested in a wave tank. The developed OWEC has a length of 1.2 m, a height of 0.45 m, and a width of 0.9 m that spans through the wave tank. The slope angle of the OWEC was fixed at 40° based on the recommendation from literature [9]. The model was fixed with a draft of 0.23 m, so its motion was not considered. Two submersible pumps were placed in the model reservoir to drain the overtopped water, mimicking the function of turbines, and measure the discharge volume and estimate the flowrate.

The model was tested in a wave flume that has dimensions of 36 m in length, 1.2 m in height, and 0.9 m in width. The tank is equipped with a programmable flap-type wave maker at one end and a sloping beach filled with horsehair at the other end, as shown in Figure 2. The tank flume doesn't have an active wave absorption system. The water depth was kept constant throughout the experiment at d = 0.80 m. The OWEC is placed at 18 m from the wavemaker while a wave gauge was placed at 1 m in front of the OWEC to measure the free surface elevations with and without the presence of the OWEC. A TI data acquisition unit is used to send out control-signals to the wavemaker and the OWEC, and to collect data-signals from wave gauges and the OWEC.

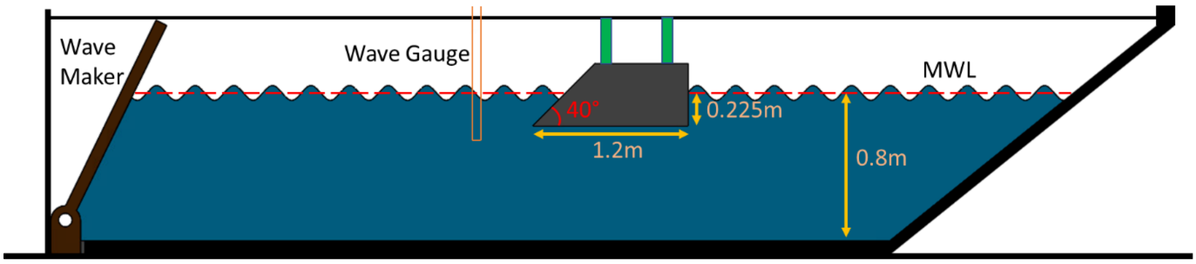

Figure 2. Sketch of the water tank and model setup (not to scale)

2.3. Smart material controlled OWEC freeboard

SMA springs were integrated as part of the model OWEC to control the freeboard length and thus R_c. The springs were controlled by controlling the electric current in them and their temperature caused by joul heating. For this purpose, power supplies were connected to the springs through electrical switches which were controlled by an electronic controller [16]. In this way, the electric current and the produced heat in the springs could be controlled. Two units of 24V and 450W switching power supplies were used in parallel to provide enough current for heating the SMA springs. In addition, a digital temperature controller with its temperature sensor alongside the contactor was used to control the current in the springs. Figures 3(a,b) shows the schematic diagram of the OWEC model and the length changing springs. For example, heating the springs by applying an electric current would shorten their length and lower the height of the ramp and R_c, as shown in 3(b). In the present model setup, 42 parallel SMA-springs were used as the actuator. This actuator, placed inside the ramp between the fixed acrylic plate and the movable plate, as shown in figure 3. The springs were connected to the acrylic boards through a copper covered aluminum ribbon, which has been used as an electrical

Preprints (www.preprints.org) | NOT PEER-REVIEWED | Posted: 8 November 2022 doi:10.20944/preprints202211.0143.v1

connector, and a mechanical holder. Besides, there are two rails between the movable board and the fixed supporting board beneath it to lower the friction. To control the temperature of the SMA-springs, the sensor was placed on one of the springs to measure the temperature and regulate it by switching on/off the current of springs using the contactor.

The cavity which is formed between the acrylic plates and contains the springs inside should be adequately sealed. The springs were sealed by using a waterproof fabric to isolate the cavity and springs from overtopping water so the springs' temperature could be successfully controlled. Figures 3(c-d) shows the SMA spring layout (between the two transparent acrylic boards) and the OWEC placed in the wave tank. Soft polymeric materials with their flexible and waterproof nature can be an alternative to provide a reliable and durable sealing to the designed OWEC [17,18].

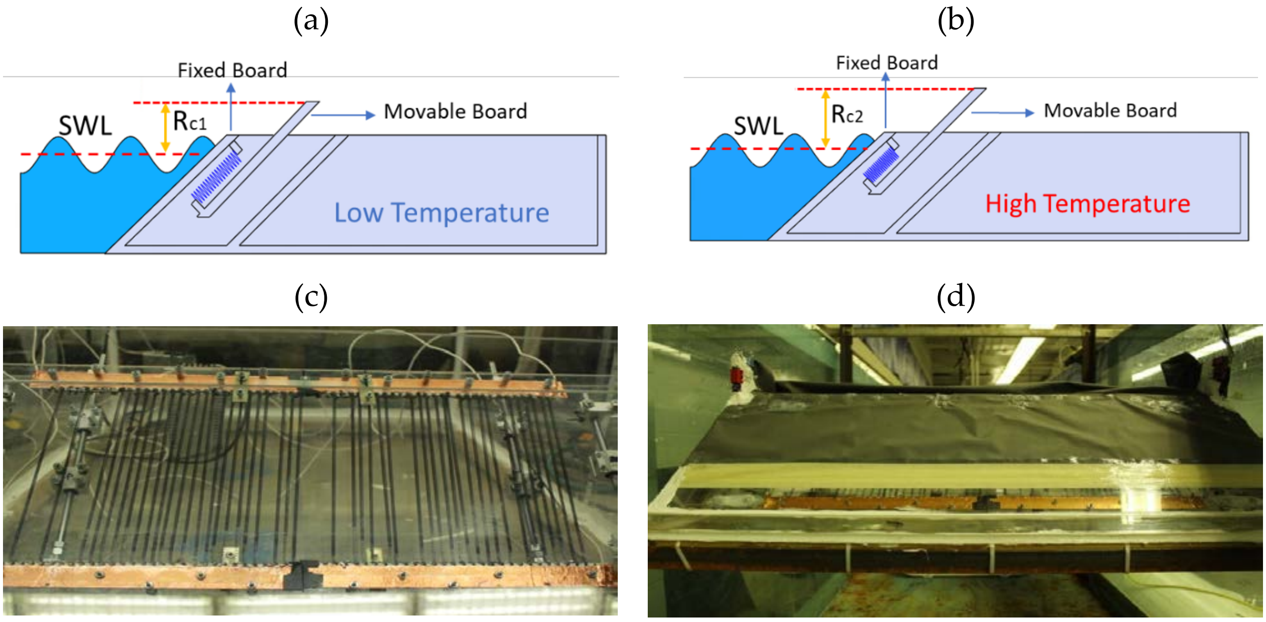

Figure 3. The SMA springs-controlled board length: (a) smaller R_c at lower temperature and (b) larger R_c at higher temperature. (c) Photo of SMA connected ramp and (d) photo of the front view of the ramp of the OWEC setup in the tank.

Precise sensors can help to control the position of the movable board and the temperature of the SMA springs more accurately [19,20]. To have a better sealing, wireless communication link can be used to transfer data from the sensor to the control unit [21,22].

3. Experimentation

To tests the effectiveness of the OWEC, the developed model was examined in various wave conditions. Irregular waves were generated by varying significant wave heights (H_s) while fixing the peak period (T_p = 1.0 s) based on the JONSWAP spectra [23]. In each wave condition, the model was tested in two ways. The first way was with a fixed R_C (R_C = 0.075 m) in which the actuator and controller were turned off, whereas the second way was with an adjustable R_c by switching on the actuator and controller. Table 1 shows the conditions of the experiment.

Preprints (www.preprints.org) | NOT PEER-REVIEWED | Posted: 8 November 2022 doi:10.20944/preprints202211.0143.v1

Figure 4 shows R_c versus adjusted temperature during the experiment. The trend in the figure is neither monotonic nor smooth when the temperature is around 45°C. This is caused by the hysteresis around the transition temperature of the SMA-springs. It means a small variation in the temperature produces a relatively large length variation at this range. The hysteresis effect in SMA phase shifting, the test environment, such as the room temperature and humidity, and friction on the rails, may all affect controlling and adjusting the ramp length and R_c in the developed model.

The ideal scenario on adjusting the R_c value through the SMA springs should be based on current or predicted wave parameters through a real-time sampling of waves and corresponding spectrum. However, because of the limited length of the wave flume and not having an active absorbing capability of the wavemaker, real-time sampling of waves and spectrum are not possible due to severe wave reflection from the OWEC and the wavemaker. Alternatively, the tests were conducted in a way that R_c was adjusted to an ideal value using the SMA springs through the temperature controller for each prescribed wave spectrum. In another word, by fixing T_p = 1.0 s, we ran the experiment 9 times for the 7 different H_s values, as shown in Table 1, with the R_c value adjusted separately in each run. The adjustable R_c results were then compared with that from repeated tests using the same wave spectra except with a fixed, constant R_c value for all the 9 spectra.

Table 1. Test conditions with fixed and adjustable R_c

Condition	R_c value (and applied temperature)
H_s	0.048 m, 0.062 m, 0.075 m, 0.089 m, 0.102 m, 0.116 m, and 0.129 m
Fixed R_c	0.075 m
Adjustable R_c	0.068 m (30°C), 0.071 m (35°C), 0.078 m (40°C), 0.090 m (47.5°C), 0.096 m (55°C), 0.102 m (45°C), 0.103 m (50°C), 0.111 m (60°C), and 0.116 m (65°C)

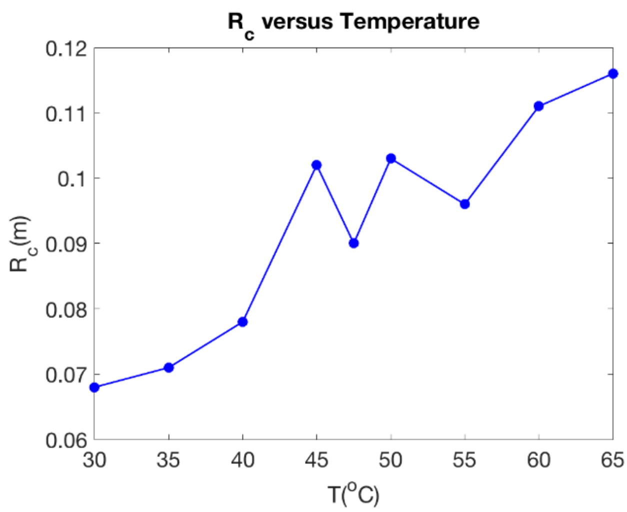

Figure 4. R_c versus applied temperature for the SMA-controlled OWEC

Preprints (www.preprints.org) | NOT PEER-REVIEWED | Posted: 8 November 2022 doi:10.20944/preprints202211.0143.v1

To minimize the wave reflection problem, the duration of each test was determined in a way that the measurements were stopped once the leading waves were re-reflected, after reflected from the OWEC, from the wavemaker and reached the OWEC. Based on the wave group velocity, the duration was determined as 68 s. However, a 68-s wave train generated from each given spectrum is too short to represent the spectrum, so three sets of 68-s wave trains were generated, in separated runs, to represent a longer duration spectral wave for each H_s case. The test results were then combined to present the outcomes from that specific spectrum. The discrepancy for the combined wave trains (of 204 s total duration) is about 3% of the target H_s value.

4. Results and Discussion

The experimental results were obtained for both the fixed R_c OWEC and the adjustable R_c OWEC. The range of the experimental data depends on R (=R_c/H_s). In the present study, when the R value is greater than 2.0, the overtopping discharge rate is too small to be accurately measured. On the other hand, when the R value is less than 0.5, the overtopping discharge rate is too large to be measured accurately [24]. Thus, the available data range is between $R = 0.5$ and $R = 2.0$. Based on the dimensions of the OWEC model, λ_{dr} is calculated as 0.919 and λ_α is 0.955. Equation (2) can thus be rewritten as.

$$Q = 0.176\lambda_s e^{-2.60\frac{R}{\gamma}} \quad (6)$$

In which λ_s is determined using Equation (5). Equation (6) was then used to compare with the overtopping discharge rate measured from the fixed R_c OWEC with a reduction factor set as $\lambda = 1$ (i.e., assuming zero roughness) to validate the overtopping rate in the present study.

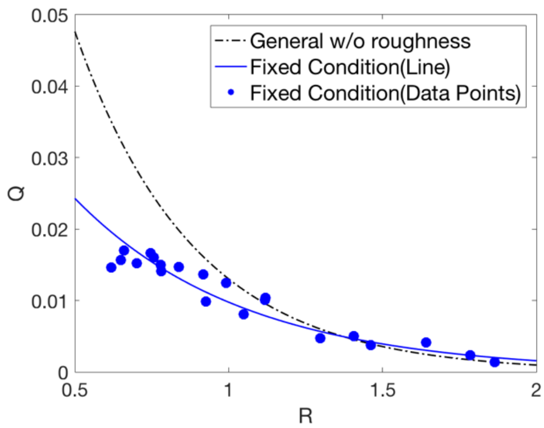

Figure 5. Comparison between the fixed R_c OWEC and Equation (6).

The result of the fixed freeboard OWEC is shown in Figure 5 (R_c = 0.075 m as shown in Table 1). By varying the H_s value in each spectrum wave train, a particular R value and corresponding Q value can be obtained, as shown in Figure 5 with 20 variations. The empirical Equation (6) was also plotted for comparison. The comparison shows some deviation at the low R values, especially when $R < 1$. It is unclear what causes the difference, but it could be due to the use of $\lambda = 1$. The zero-roughness assumption may be correct since the ramp is made of acrylic. Nevertheless, the sandwiched ramp (for inserting the SMA springs in between the plates) and the use of fabric to seal it may cause extra equivalent roughness. The difference becomes negligible if the λ value is lowered to 0.925, but that is arbitrary, so it was not used here in the plot.

To test the OWEC with the adjustable R_c, the SMA springs and controller were powered on and nine different temperatures were chosen, as shown in Table 1, for nine different heights of R_c under various H_S values. The purpose of these experiments is to validate that the OWEC with adjustable R_c is comparable with the OWEC with fixed R_c, and changing R_c does not adversely alter the overtopping discharge rate shown in figure 5. Note that the test range covers only $R \geq 0.5$ in the present study and in most other similar studies, mainly due to the difficulty of measuring Q correctly in such a violent overtopping and splashing flow caused by the very low R_c to H_S ratio.

In figure 6(a), the results for the OWEC with adjustable R_c are plotted. The 58 data points seem to follow an exponential trend line well with relatively minor deviations. In figure 6(b), the results from the adjustable freeboard tests in Figure 6(a) are replotted together with the results of the fixed freeboard tests in figure 5. The figure shows that both the fixed and adjustable freeboard OWECs resulted in agreeable overtopping discharge results, although there exists certain discrepancy in the lower R region.

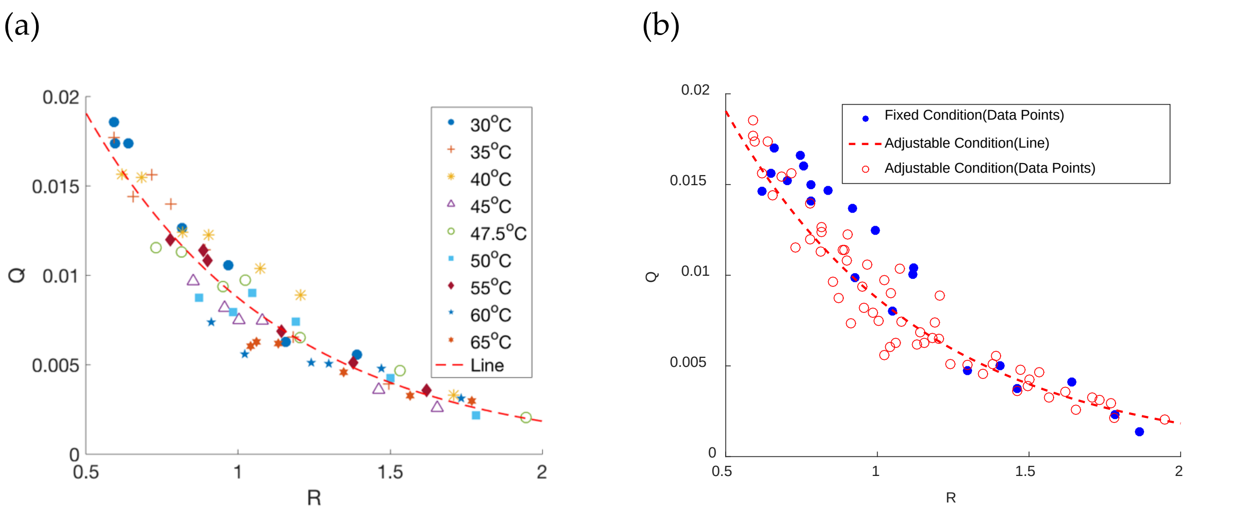

Figure 6. Experimental results for OWEC with adjustable R_c. (a) All the data points with the different values of temperature. The regression line $Q = 0.0416e^{-1.56R}$ has an R^2 value of 0.93. (b) Comparison between the OWEC with fixed R_c and OWEC with adjustable R_c.

As shown in Figure 6(b), the adjustable R_c OWEC is capable of reproducing about the same Q values in comparison to the fixed R_c OWEC. We may then use that to examine how much higher magnitude of Q an adjustable R_c OWEC can produce over the corresponding fixed R_c OWEC. By using an optimal R value that has been known to produce the highest Q, the adjustable OWEC may adjust its ramp height based on the H_s value of the incoming wave spectrum to maximize its overtopping discharge rate.

Preprints (www.preprints.org) | NOT PEER-REVIEWED | Posted: 8 November 2022 doi:10.20944/preprints202211.0143.v1

To quantify the improvement of the adjustable R_c OWEC over the fixed R_c OWEC, we used the ideal $R = R_c/H_s = 0.5$ condition for the 7 cases of different H_s listed in Table 1. Each significant wave height case in the laboratory conditions was numerically simulated for one hour. For the fixed R_c OWEC, the average wave height of the 7 combined significant wave heights was used, i.e., the resulting H_s for the combined spectrum wave trains is 0.0927 m. Accordingly, the desired R_c is 0.0464 m. That results in $R = 0.5$ and maximize the Q value for the fixed R_c OWEC. On the other hand, for the adjustable R_c OWEC, the R value is set as 0.5 for each significant wave height, meaning that the R_c value is changed each hour. Table 2 shows the comparison with Q calculated using the regression line in Fig. 6. Note that the last two rows in the table were not used in the comparison because the regression line in Fig. 6 only covers $R \geq 0.5$. Based on the table, the adjustable R_c has an 16% increase of overtopping discharge than the fixed condition (i.e., a flowrate of 5.426 L/s versus 6.302 L/s as shown in Table 2). 16% improvement in efficiency for the present laboratory scale tests was achieved. In real oceans the increment of efficiency likely depends on the spectra width and hourly height variation. A more significant advantage in efficiency is likely to be achieved when the adjustable R_c OWEC is placed in a wave environment featuring a wider spectral band [25,26].

Table 2. Flowrate comparison between fixed R_c OWEC and adjustable R_c OWEC in lab scale

	Fixed R_c					Adjustable R_c				
H_s (m)	R_c (m)	R (-)	Q (-)	*Flowrate* (L/s)	*Discharge* (10^3 L)	R_c (m)	R (-)	Q (-)	*Flowrate* (L/s)	*Discharge* (10^3 L)
0.048	0.046	0.97	0.0092	0.303	1.09	0.024	0.50	0.0191	0.627	2.26
0.062	0.046	0.75	0.0129	0.626	2.25	0.031	0.50	0.0191	0.921	3.32
0.075	0.046	0.62	0.0158	1.019	3.67	0.038	0.50	0.0191	1.226	4.41
0.089	0.046	0.52	0.0184	1.534	5.52	0.045	0.50	0.0191	1.584	5.70
0.102	0.046	0.50	0.0191	1.944	7.00	0.051	0.50	0.0191	1.944	7.00
0.116	0.046	0.40	-	-	-	0.058	0.50	0.0191	2.357	8.49
0.129	0.046	0.36	-	-	-	0.065	0.50	0.0191	2.765	9.95
Sum ($R\geq0.5$ in rows 1 to 5)				5.426	19.53				6.302	22.69

5. Concluding Remarks

A new concept of using SMA-based actuator to adjust the freeboard crest height of an OWEC is demonstrated. This new OWEC design can change its freeboard height R_c automatically to harvest energy more efficiently from time-varying wave condition. A scaled model was built and tested in the laboratory to proof the new concept and verify the efficiency improvement. The crest freeboard height was varied by controlling the temperature of SMA springs and thus the length of the springs. Verification of the adjustable OWEC with a fixed OWEC was performed to ensure the two OWEC are essentially functioning the same. The adjustable OWEC was then used to explore how much increment of energy harvesting efficiency it may be able to gain. Based on the obtained empirical formulas for overtopping flowrate, several virtual sea states in laboratory scale were artificially tested with each sea state lasted for an hour to calculate the overtopping discharge. The comparison shows that the proposed adjustable OWEC can improve the overtopping flowrate by 16%. However, the efficiency may also depend on how the sea states change and the spectrum of the waves.

The controlling of the freeboard length needs to be more precise and consistent to achieve a higher efficiency. That is especially important if the concept is going to be applied in the prototype. Furthermore, a closed loop feedback system to adjust the freeboard length and height automatically based on the ambient wave condition as well as an onboard prediction system for upcoming wave condition is essential to have a real-time adjustment in R_c.

Acknowledgments

This study was supported by the Texas A&M Energy Institute through a project titled "Development of Synergetic/mobile Multi-source Multi-purpose Ocean Renewable Energy Station."

References

[1] S. Baghbani Kordmahale, J. Do, K.-A. Chang, and J. Kameoka, "A Hybrid Structure of Piezoelectric Fibers and Soft Materials as a Smart Floatable Open-Water Wave Energy Converter," *Micromachines*, vol. 12, no. 10, p. 1269, 2021, doi: 10.3390/mi12101269.

[2] S. Baghbani Kordmahale, J. Do, K. A. Chang, and J. Kameoka, "Low Cost and Piezoelectric based Soft Wave Energy Harvester," *MRS Adv.*, vol. 4, no. 15, pp. 889–895, 2019, doi: 10.1557/adv.2018.675.

[3] P. Frigaard, J. Tedd, J.P. Kofoed, and E. Friis-Madsen, " 3 Years Experience with Energy Production on the Nissum Bredning Wave Dragon Prototype," In Proceedings of the Fourth CA-OE Workshop: Performance Monitoring of Ocean Energy Systems, Lisbon, 16-17 November, 2006 Coordination Action on Ocean Energy (CA-OE) : Sixth Framework Programme.

[4] J. W. Van der Meer, and J. P. Janssen "Wave run-up and wave overtopping at dikes and revetments." Delft Hydraulics, no.485, pp.1-22 Delft, the Netherlands, Aug 1994.

[5] J.W. Van der Meer "Technical report wave run-up and wave overtopping at dikes." Colophon Publication, Technical Advisory Committee on Flood Defense, Delft, the Netherlands, May 2002.

[6] N. J. Shankar and M. P. R. Jayaratne, "Wave run-up and overtopping on smooth and rough slopes of coastal structures," *Ocean Eng.*, vol. 30, pp. 221–238, 2003.

[7] T. Bruce, J. W. Van Der Meer, L. Franco, and J. M. Pearson, "Overtopping performance of different armour units for rubble mound breakwaters," *Coast. Eng.*, vol. 56, no. 2, pp. 166–179, 2009, doi: 10.1016/j.coastaleng.2008.03.015.

[8] J.P. Kofoed "Wave Overtopping of Marine Structures: utilization of wave energy." Hydraulics & Coastal Engineering Laboratory, Department of Civil Engineering, Aalborg University, 2002.

[9] A. Nielsen, and J. P. Kofoed (1997). "The Wave Dragon: evaluation of a wave energy converter." Department of Civil Engineering, Aalborg University, 1997.

[10] V. Lander, P. Troch, and J. P. Kofoed, "On the Effects of Geometry Control on the Performance of Overtopping Wave Energy Converters," *Energies*, vol. 4, pp. 1574–1600, 2011, doi: 10.3390/en4101574.

[11] J. Tedd, "Testing, analysis and control of the wave dragon wave energy converter." Department of Civil Engineering, Aalborg University,2007.

[12] J. M. Jani, M. Leary, A. Subic, and M. A. Gibson, "A review of shape memory alloy research , applications and opportunities," *Mater. Des.*, vol. 56, pp. 1078–1113, 2014, doi: 10.1016/j.matdes.2013.11.084.

[13] S. Baghbani Kordmahale and J. Kameoka, "Smart Soft Actuation System," *Ann. Mater. Sci. Eng.*, vol. 2, no. c, pp. 2–3, 2015, [Online]. Available: https://austinpublishinggroup.com/material-science-engineering/fulltext/amse-v2-id1021.php.

[14] DYNALLOY, I.. "FLEXINOL® Actuator Spring Technical and Design Data." from http://www.dynalloy.com/tech_data_springs.php (2021)

[15] C. Zhang, R.H. Zee, P.E.Thoma, "Development of Ni-Ti based shape memory alloys for actuation and control." Energy Conversion Engineering Conference, Proceedings of the 31st Intersociety, IEEE, 1996.

[16] P.-J. Huang, S. Baghbani Kordmahale, C.-K. Chou, H. Yamaguchi, M.-C. Hung, and J. Kameoka, "Development of automated high throughput single molecular microfluidic detection platform for signal transduction analysis," in *SPIE 9705, Microfluidics, BioMEMS, and Medical Microsystems XIV*, vol. 9705, pp. 1–5, doi: 10.1117/12.2213259.

[17] D. Steck, J. Qu, S. Baghbani Kordmahale, D. Tscharnuter, A. Muliana, and J. Kameoka, "Mechanical responses of Ecoflex silicone rubber : Compressible and incompressible behaviors," *J. Appl. Polym. Sci.*, vol. 136, no. 5, pp. 1–11, 2019, doi: 10.1002/app.47025.

[18] S. Baghbani Kordmahale, J.Qu, A.H. Muliana, and J.Kameoka, " A Hydraulic Soft Microhand with an Application of Live Insect Manipulation," 14 September 2021, PREPRINT (Version 1) available at Research Square [https://doi.org/10.21203/rs.3.rs-899495/v1]

[19] S. Rezaie, Z. G. Bafghi, N. Manavizadeh, and S. Baghbani Kordmahale, "Highly Sensitive Detection of Dissolved Gases in Transformer Oil With Carbon-Doped ZnO Nanotube : A DFT Study," *IEEE Sens. J.*, vol. 22, no. 1, pp. 82–89, 2022.

[20] M. Khurana, S. Baghbani Kordmahale, C. Bowerman, X. Liu, and A. Akimov, "3D nano-printing coupler for silicon nitride suspended waveguide," in *Proc. SPIE 12012, Advanced Fabrication Technologies for Micro/ Nano Optics and Photonics XV*, 2022, vol. 1201209, no. March, pp. 1–3, doi: 10.1117/12.2608393.

[21] A. P. Saghati, S. Baghbani Kordmahale, J. Kameoka, and K. Entesari, "Reconfigurable Quarter-Mode Substrate Integrated Waveguide Cavity Filter Employing Liquid-Metal Capacitive Loading," in *2015 IEEE MTT-S International Microwave Symposium*, 2015, pp. 20–22, doi: 10.1109/MWSYM.2015.7166885.

[22] A. P. Saghati, S. Baghbani Kordmahale, A. P. Saghati, J. Kameoka, and K. Entesari, "Reconfigurable quarter-mode SIW antenna employing a fluidically switchable via," in *2016 IEEE Antennas and Propagation Society International Symposium, APSURSI 2016 - Proceedings*, 2016, no. June, pp. 845–846, doi: 10.1109/APS.2016.7696131.

[23] K. Hasselmann, T.P.Barnett, E.Bouws, H.Carlson, et al. "Measurements of wind wave growth and swell decay during the Joint North Sea Wave Project (JONSWAP)." Hydraulic Engineering Reports, Deutches

 doi:10.20944/preprints202211.0143.v1

Hydrographisches Institut, 1973.

[24] J.Juhl, and P. Sloth “Wave overtopping of breakwaters under oblique waves.” 24th International Conference on Coastal Engineering, October 23-28, 1994, Kobe, Japan, pp. 1182-1196

[25] T. Sakakiyama, and R. Kajima, “Wave overtopping and stability of armor units under multidirectional waves. 25th International Conference on Coastal Engineering, September 2-6, 1996, Orlando, Florida, United States, pp. 1862-1875

[26] H.Schüttrumpf, J. Moller, H.Oumeraci, J.Grune, and R.Weissmann, “Effects of natural sea states on wave overtopping of sea dikes.” Fourth International Symposium on Ocean Wave Measurement and Analysis, September 2-6, 2001, San Francisco, California, United States, pp. 1565-1574